Kinesin-Recruiting Microtubules Exhibit Collective Gliding Motion While Forming Motor Trails

Stanislav Tsitkov[1], Yuchen Song[1,2], Juan B. Rodriguez III[1], Yifei Zhang[1], Henry Hess[1*]

1. Department of Biomedical Engineering, Columbia University, New York, NY 10027, United States
2. Department of Biomedical Engineering, Hong Kong Polytechnic University, Hong Kong SAR, China

*Corresponding Author: hh2374@columbia.edu

ABSTRACT: Microtubules gliding on surfaces coated with kinesin motors are minimalist experimental systems for studying collective behavior. Collective behavior in these systems arises from interactions between filaments, *e.g.* from steric interactions, depletion forces or cross-links. To maximize the utilization of system components and the production, it is desirable to achieve mutualistic interactions leading to the congregations of both types of agents, that is cytoskeletal filaments and molecular motors. To this end, we used a microtubule-kinesin system, where motors reversibly bind to the surface *via* an interaction between a hexahistidine (His_6) tag on the motor and a Ni(II) – nitrilotriacetic acid (Ni-NTA) moiety on the surface. The surface density of binding sites for kinesin motors was increased relative to our earlier work driving the motors from the solution to the surface. Characterization of the motor-surface interactions in the absence of microtubules yielded kinetic parameters consistent with previous data and revealed the capacity of the surface to support two-dimensional motor diffusion. The motor density gradually fell over two hours, presumably due to the stripping of Ni(II) from the NTA moieties on the surface. Microtubules gliding on these reversibly bound motors were unable to cross each other and at high enough densities began to align and form long, dense bundles. The kinesin motors accumulated in trails surrounding the microtubule bundles and participated in microtubule transport.

KEYWORDS microtubules, kinesin, collective motion, nematic alignment, hexahistidine tag, surface diffusion, mutualistic interactions

Swarming organisms, such as flocks of birds, schools of fish, and tuxedos of penguins self-organize and respond to environmental stimuli through inter-agent interactions.[1-7] Advances in robotic technology[8-10] and synthetic biology[11-16] create a need for a fundamental understanding of how collective behaviors emerge as a function of the actions and interactions of individual agents;[17] it would allow for better design in applications ranging from drug delivery by colonies of magneto-tactic bacteria, over directing traffic flow of fleets of self-driving cars, to aerial control of gaggles of drones.[16, 18-20] Systems of active nanoscale filaments, such as functionalized microtubules propelled by surface-adhered kinesin motor proteins,[21-29] are excellent testbeds for analyzing how simple interactions between agents result in dynamic self-assembly and collective behaviors.[30-43] One of the first systems described consisted of biotinylated microtubules gliding on a kinesin-1 motor protein-coated surface, which cross-link *via* biotin-streptavidin bonds and form spools and wires.[37, 44-46] Under optimal conditions nearly millimeter-long wires can form.[38] Microtubules gliding on kinesin motors in the presence of weaker, depletion force-induced interactions have been shown to form nematically organized streams.[34-36, 39, 40] Microtubules gliding on truncated kinesin motors in the absence of depletion forces exhibited collective behavior dependent on kinesin surface density; these behaviors varied from long range order at low kinesin densities to clustering at high kinesin densities.[41] Actin filaments gliding on myosin motors in the presence of depletion forces have been demonstrated to form streams and density waves, and have been used to test theories of active matter.[30, 32, 33, 47] Microtubules gliding on dynein-coated surfaces have been found to nematically align upon collisions, resulting in the formation of large vortices.[43]

These nanorobotic and active matter systems are constructed in a way that prevents the utilization of a large portion of the available components: the majority of the biomolecular motors attached to the surface are idly standing by, rather than actively propelling filaments. If motors could co-localize with cytoskeletal filaments, the utilization of system components and other benefits arising from motor-filament interactions, such as enhanced

filament stability,[48, 49] would be maximized. Such a mutualistic interaction[50] between motors and filaments would be reminiscent of how the spread of fruit seeds by elephants leads to the growth of fruit-bearing trees along their paths.[51-53] Our goal was to engineer such a mutualistic interaction in the microtubule-kinesin system (Figure 1a).

A first step towards that goal was to develop a system where motors could dynamically change their position, turning them into mobile agents. This was achieved in our previous work that described a system consisting of microtubules gliding on reversibly surface-adhered kinesins (Figure 1b).[54, 55] Reversibility arises from a weak interaction between kinesins and the surface *via* Ni-NTA – His-tag bonds (Figure 1b).[54] A microtubule gliding on the surface accumulates kinesin motors from solution, places them on the surface in a "trail" under itself, and uses them to propel itself forward. After kinesins have reached the end of a microtubule they are left behind, and unbind from the surface within a minute. As such, kinesin motors undergo reversible transitions between four states: (1) diffusing in solution, (2) head-bound to a microtubule, (3) tail-bound to the surface, and (4) doubly-bound to both the microtubule and the surface (Figure 1c). The earlier experiments did not demonstrate collective behavior, due to low microtubule densities and weak interactions between microtubules. An important shortcoming of the system was that, due to the weak binding to the surface, 99% of the kinesin motors were diffusing in the solution without contributing to the generation of force.

Here, a regime of this dynamic system is demonstrated, where the density of Ni-NTA binding sites on the surface is hundred-fold increased and the kinesin population is shifted towards the surface-bound states (states (2) and (4) in Figure 1c). In this regime gliding microtubules exhibit collective behavior by assembling into dense bundles (Figure 1d). Bundling arises from a higher microtubule density and a direct, steric interaction discouraging microtubules from crossing due to a strong, kinesin-mediated microtubule-surface interaction, similar to that observed by Tanida *et al.*[41] Kinesin motors are initially dispersed on the surface, but increasingly co-localize with the microtubule bundles. The resulting bundles provide not only a demonstration of mutualistic collective behavior in a system of two mobile agents, but also demonstrate the possibility of higher order self-assembly where both motors and filaments assemble hierarchically.

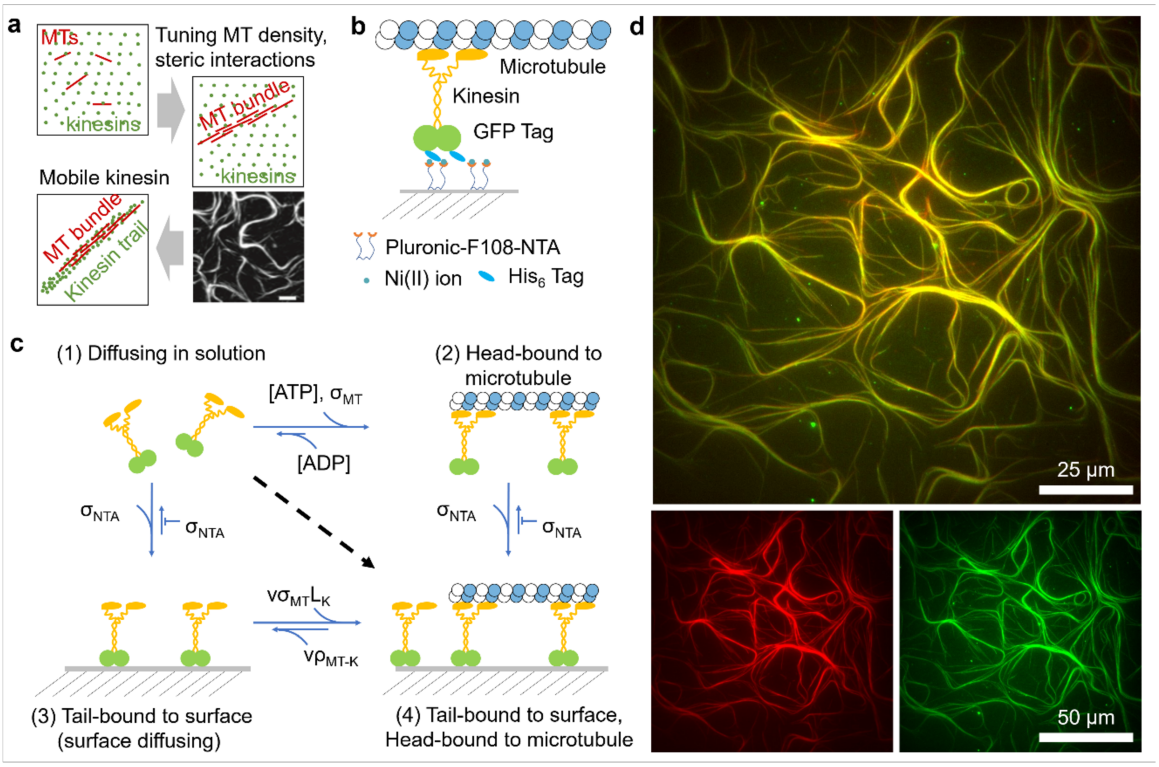

Figure 1. Studying collective behavior in the microtubule/kinesin system with reversible kinesin binding. (a) In the traditional microtubule-kinesin system, microtubules glide on surfaces uniformly coated with kinesin motors. By tuning the microtubule density and steric interactions, Tanida *et al.*[41] demonstrated that this system can be used to generate dense bundles (scale bar 20 μm). (Image reprinted with permission from Tanida *et al.*[41]. Copyright 2020 American Physical Society). We engineer a system where kinesin motors dynamically reorganize to co-localize with microtubules. (b) Schematic of the kinesin-surface bond. In our dynamic system, kinesin motors labeled with green fluorescent protein (GFP-kinesin) and tagged with a His_6 tag reversibly bind to the Pluronic-F108-NTA coated surface *via* a weak, His_6-Ni-NTA bond. (c) Schematic of motor binding states. In our dynamic system, motors can access four states: diffusing in solution, head-bound to a microtubule, tail bound to the surface, and both head-bound to a microtubule and tail bound to the surface. The fluxes between these states

strongly depend on ATP concentration ([ATP]), microtubule surface density (σ_{MT}), and kinesin surface binding site density (σ_{NTA}). The parameters L_K and $\rho_{MT\text{-}K}$ denote the reach length of kinesin and kinesin linear density along the microtubule, respectively. (d) (Top) Composite images of HiLyte 670 microtubules (red) and GFP-kinesin motors (green) imaged using total internal reflection fluorescence (TIRF) microscopy. (Bottom) Individual channels showing the formation of bundles of HiLyte 670 microtubules (red) and trails of GFP-kinesin motors (green). Images taken 30 mins after the start of the experiment; the initial experimental conditions were 1 mM ATP, 25 nM GFP-Kinesin, and 16 μg/mL tubulin.

Results and Discussion

Dynamics of the kinesin-surface interaction in the absence of microtubules

Although stable microtubule gliding was achieved in the demonstration of this dynamic system by Lam *et al.*[54], its analysis revealed that the interaction of GFP-kinesin motors with the surface was weaker than expected: the association constant of GFP-kinesin binding to the surface was 0.3 μm^{-2} nM^{-1}, which implied a Ni-NTA binding site surface density of 300 μm^{-2}, (based on the 1 μM dissociation constant for the NTA-His_6 bond accepted in literature[56, 57]) a value far below the maximum packing density of 62,500 μm^{-2} (considering a radius of gyration of about 2 nm for the Pluronic F108-NTA polymer). The presence of imperfections in the coating was further highlighted by high densities of non-specifically bound kinesin aggregates on the surface.

Here, the strength of the motor-surface interaction was increased by adopting a rigorous coverglass cleaning procedure, which included an acetone wash, a base etch, and a longer silanization step. Furthermore, in order to lessen the stripping of Ni(II) ions from the surface, dithiothreitol (DTT) was removed from the oxygen scavenging system, and the Ni(II) ion concentration in the 2 mg/mL Pluronic F108-NTA coating solution was increased from 50 mM $NiSO_4$ to 500 mM $NiSO_4$. The removal of DTT did not appear to have a significant effect on photobleaching. The implementation of this cleaning procedure changed the dynamics of the interaction of GFP-kinesin with the Pluronic F108-NTA-coated surface.

The kinesin-surface interaction was characterized in experiments where kinesin motors interacted with the surfaces in the flow cell in the absence of microtubules (Figure 2a). Single molecule imaging of picomolar quantities of GFP-kinesins interacting with the surface were used to calibrate the fluorescence signal as a function of microscope, and camera settings and exposure time (Supplementary Section 1).

The surface density of kinesin motors changed with time, increasing from 0 μm^{-2} to 1200 μm^{-2} within the first 500 seconds of the experiment and then falling to 500 μm^{-2} within the next 1,500 seconds (Figure 2a-c). The slow rise in surface density can be attributed to the diffusion-limited landing rate of motors on the surface; the subsequent depletion of motors from the surface can be explained by the stripping of nickel ions from the surface by ethylene glycol tetraacetic acid (EGTA) molecules in the BRB80 buffer (Figure 2b-c). Two different models incorporating mass transport-limited surface kinetics were used to fit the data: a two-compartment model which is commonly used to analyze data from signal plasmon resonance (SPR) experiments for binding kinetics,[58, 59] and a landing rate model approximating the diffusion equation with reversible surface binding[60] (Supplementary Section 2).

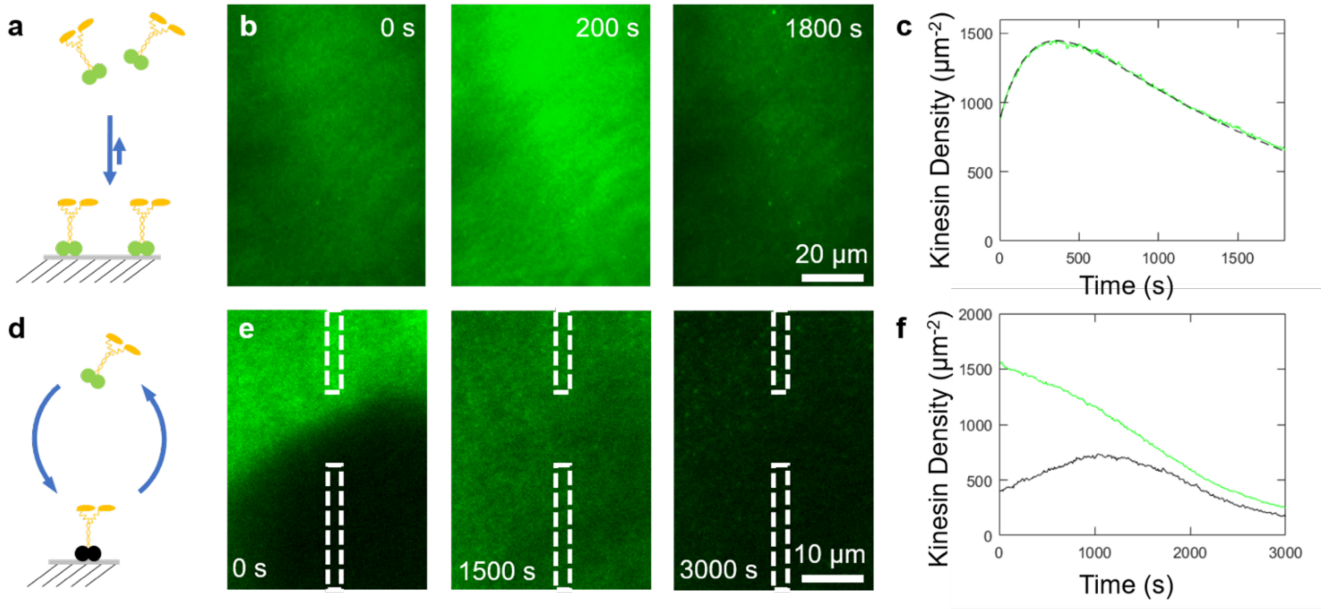

Figure 2. The kinesin-surface interaction *via* the NTA-His_6 bond is dynamic even in the absence of microtubules. (a) The binding of GFP-kinesin motors to the surface is observed *via* fluorescence imaging with TIRF illumination. (b) Images of

the surface at identical contrast settings taken at 0 s, 200 s, and 1800 s after the beginning of the experiment show a clear peak in fluorescence near 200 s. (c) Average kinesin density over time (green) fit with a two-compartment model (black, dashed) describing mass-transfer limited adsorption of kinesin motors to the surface. Details on the calibration are in the Supplementary Info. (d) In a Fluorescence Recovery After Photobleaching (FRAP) experiment a region of the field of view is photobleached, and the recovery of fluorescence in the bleached region is observed and compared to that of a nearby unbleached region. (e) Images taken 0 s, 1500 s, and 3000 s after photobleaching, and (f) profile of fluorescence of unbleached area (green) and bleached area (black) obtained from the indicated areas as described in Supplementary Section 4.

While the models have different forms, they arrive at similar conclusions: The association constant for the motor-surface interaction is between 60-100 μm^{-2} nM^{-1}, which implies a Ni-NTA surface density of 60,000-100,00 μm^{-2} (based on the accepted K_D of 1 μM for the NTA-His_6 interaction), a value which is much closer to the packing density and compares well to SPR measurements of the Pluronic-F108 coating density on a gold surface of 58,000 μm^{-2}.[61] The rate constant for the decrease of the motor surface density at the longer time scale (>500 s) is $6 \cdot 10^{-4}$ s^{-1}, presumably due to the stripping of Ni(II) ions from the surface by the 2 mM EGTA (a chelator for divalent ions) in the BRB80 buffer. This stripping rate is comparable to the $1.7 \cdot 10^{-4}$ s^{-1} rate found by Nieba *et al.*[56] for His-tagged streptavidin leaving a Ni-NTA Bioacore surface in the presence of 300 μM EDTA and the $3 \cdot 10^{-4}$ s^{-1} stripping rate for hexahistidine peptides leaving a Ni-NTA coated surface in the experiments of Knecht *et al.*[57] Nickel ion stripping was also observed in a similar assay examining microtubule gliding on a tris-NTA coated surface by Bhagawati *et al.*[62] We ensured that the fall in fluorescence was not due to photobleaching by observing that unexposed regions of the surface 200 μm away had similar fluorescence. The surface density of motors stopped falling after 5000 s (Supplementary Section 3), at which point it reaches a steady state value of 180 ± 40 μm^{-2} (N=7, Standard Error).

To ensure that the reversible binding of the motors was still operational while the motor density was falling, a fluorescence recovery after photobleaching (FRAP) experiment (Figure 2d-f) was performed. The recovery of fluorescence in the bleached area was compared to that of an unbleached area 20 μm away. It was found that while the fluorescence of the unbleached portion of the surface was steadily falling, the fluorescence of the bleached area initially increased, and then fell to match the diminishing intensity of the unbleached area. The ability of the surface to recover fluorescence after photobleaching indicates that the surface-kinesin interaction remains specific and reversible.

The unbinding rate of the kinesin from the surface was determined by single molecule imaging of individual GFP-kinesins landing and leaving the surface (Supplementary Section 5). 90% of the binding events identified by the tracking program had off-rates greater that 0.12 s^{-1}. This could correspond to the His_6-Tag-mono-NTA off rate constant of 1.8 s^{-1} found be Lata *et al.*[63]; however, the accuracy of this estimate is limited by the minimum 0.5 s exposure time necessary to image the single fluorophore and also limited by the false-positive rate of the automation of the tracking program. 10% of tracked kinesin motors unbind from the surface with an off rate of 0.024 s^{-1}, which is in excellent agreement with the experimentally determined off-rate for His_6-Tag-bis-NTA binding of 0.022 s^{-1} found by Lata *et al.*[63]

An additional interesting behavior observed in these single molecule experiments was the surface diffusion of individual motors (Supplementary Section 5). By fitting their mean square displacement (MSD) with $MSD = 4D\Delta t + c$, it was found that GFP-kinesins had a surface diffusion coefficient of $(1.70 \pm 0.02) \cdot 10^{-3}$ μm^2 s^{-1}, which is surprising because a surface density of binding sites on the order of 60,000 μm^{-2} and an off rate as high as 1.8 s^{-1} would imply a surface diffusion coefficient of $3 \cdot 10^{-5}$ $\mu m^2/s$, suggesting that the movement of individual fluorophores is due to either displacement reactions or crawling mechanisms.[64, 65]

Dynamics of microtubule motility

In pursuit of our goal to enhance microtubule interactions as they are propelled by the kinesin on the surface, we increased the microtubule surface density five-fold relative to Lam *et al.*[54] to 14,000 mm^{-2}. The microtubules had an average length of 21 ± 1 μm and were gliding in the presence of 25 nM GFP-kinesin and an initial ATP concentration of 1 mM (initial velocity: 610 ± 10 nm/s). The microtubule density was chosen such that the rate of collisions between microtubules (proportional to the microtubule density σ, length l, and velocity v: $k_{interaction} \sim \sigma l v$) was roughly an order of magnitude larger than the rate at which a gliding microtubule loses directional information (proportional to velocity and inversely proportional to a trajectory persistence length L_P: $k_{persistence} \sim v/L_P$). This gives a critical density of $\sigma_{crit} \approx 1/L_P l = 500\ mm^{-2}$ for 20 μm-long microtubules with a trajectory persistence length of 100 μm.[66] The microtubules surface density used by us is similar to the 50,000 mm^{-2} used to form vortex lattices on dynein-coated surfaces[43] and an order of magnitude smaller than the 280,000 mm^{-2} critical density determined for microtubules gliding in the presence of methylcellulose-induced depletion forces to demonstrate ordered behavior.[40]

Under these conditions, we observe microtubule bundle assembly driven by the nematic alignment of microtubules upon collisions (Figure 1d). However, due to the rapid conversion of ATP by the 25 nM kinesin (at a rate of up to 2 μM/s), the gliding velocity begins to fall within the first 10 min of the experiment. We therefore increased the initial ATP concentration to 10 mM and imaged the dynamics over the course of 2 hours, during which the microtubule velocity had fallen from an initial 720 ± 20 nm/s down to 16 ± 1 nm/s. During this time period, gliding microtubules formed

bundles and kinesin motors were redistributed from the surface to the microtubules (Figure 3a). This redistribution of kinesin can be observed in the composite images of the microtubule and kinesin channels. In these images, the color of individual microtubules changes from red at time t = 0 s to yellow at t = 7000 s. At the same time, the green background of kinesin fluorescence vanishes.

The temporal evolution of the distribution of kinesin and microtubules on the surface was quantified by recording the pixel-wise mean and variance of the flattened images of the microtubule and kinesin channels. The means of both channels remain roughly constant over time, indicating that the numbers of microtubules and kinesins remain constant (Supplementary Section 6). However, the ratio of variance to mean (Figure 3b) – often employed as a measure of swarming[67] – shows a noticeable increase after 1 h. This increase is more striking in the green channel, as motors transition from being homogenously distributed across the surface to being concentrated along the microtubules. The transition is less apparent in the microtubule channel because even the initial, disordered distribution of microtubules has a high variance due to their rod-like shape. By fitting the pixel-wise green channel fluorescence as a linear function of the pixel-wise red channel fluorescence, it is possible to decompose the fluorescence of the green channel into a background and microtubule-bound component (Figure 3c). The rate constant for background depletion is $2 \cdot 10^{-4}$ s^{-1}, similar to the $6 \cdot 10^{-4}$ s^{-1} stripping rate constant found for kinesin leaving the surface in the microtubule-free assay described in the previous section, suggesting that as the kinesin is finding fewer binding sites on the surface, it accumulates on the microtubules.

The temporal evolution of the velocity of the microtubules is shown in Figure 3d, where the average velocity of 10 microtubules was recorded every 100 frames and fit with a model accounting for the Michaelis-Menten dependence of kinesin activity on ATP concentration and the resulting ATP depletion. The fit parameters were a K_M of 1.8 mM, a v_{max} of 920 nm/s, and an active kinesin concentration of 24 nM. The high K_M value originates from the accumulation of ADP and P_i in the solution as a result of ATP hydrolysis, because ADP acts as an inhibitor.[68] Microtubule velocity can also be affected by the mechanical coupling of surface-bound motors and crowding of motors along individual microtubules, which is not modeled here.[69, 70] The high concentration of active kinesin (95 % of all kinesins), demonstrates that almost all kinesins are stepping on microtubules, because kinesin ATPase activity is dependent on microtubule binding.[71]

The drastic increase in microtubule bundling and kinesin colocalization with microtubules after one hour coincides with a significant decrease of the gliding velocity (Fjgure 3b,c). The decreasing kinesin velocity combined with a largely unchanged run length of the kinesin (Supplementary Section 7) yields a greatly reduced unbinding rate from the microtubule (as low as 0.009 s^{-1} based on a FRAP experiment). A decreasing unbinding rate from microtubules in turn stabilizes the kinesin population on the microtubules relative to the kinesin population on the surface.

The idea that longer-lasting kinesin-microtubule interactions are conducive to bundling is further supported by experiments with an additional 100 μM adenylyl-imidodiphosphate (AMP-PNP), which acts as a non-hydrolyzable analog of ATP and locks kinesin motors in the microtubule-binding ATP-bound state. This system demonstrated nematic alignment at the onset of the experiment but featured a noticeable increase in the number of spool-like bundles (Supplementary Section 8). Similar spool-like bundles have been observed by Tanida *et al.*[41] for microtubules gliding on high surface densities of kinesin, indicating that the AMP-PNP-induced spools we observe could be a consequence of a stronger microtubule-surface interaction mediated by kinesins.

The effects of varying the kinesin and microtubule concentrations are shown in Supplementary Section 9. Increasing the kinesin concentration from 25 nM to 75 nM did not have a significant effect on microtubule dynamics. However, decreasing the kinesin concentration to 3.1 nM prevented bundle formation and lowered microtubule surface-landing. Decreasing microtubule density two-fold and ten-fold resulted in less dense bundles.

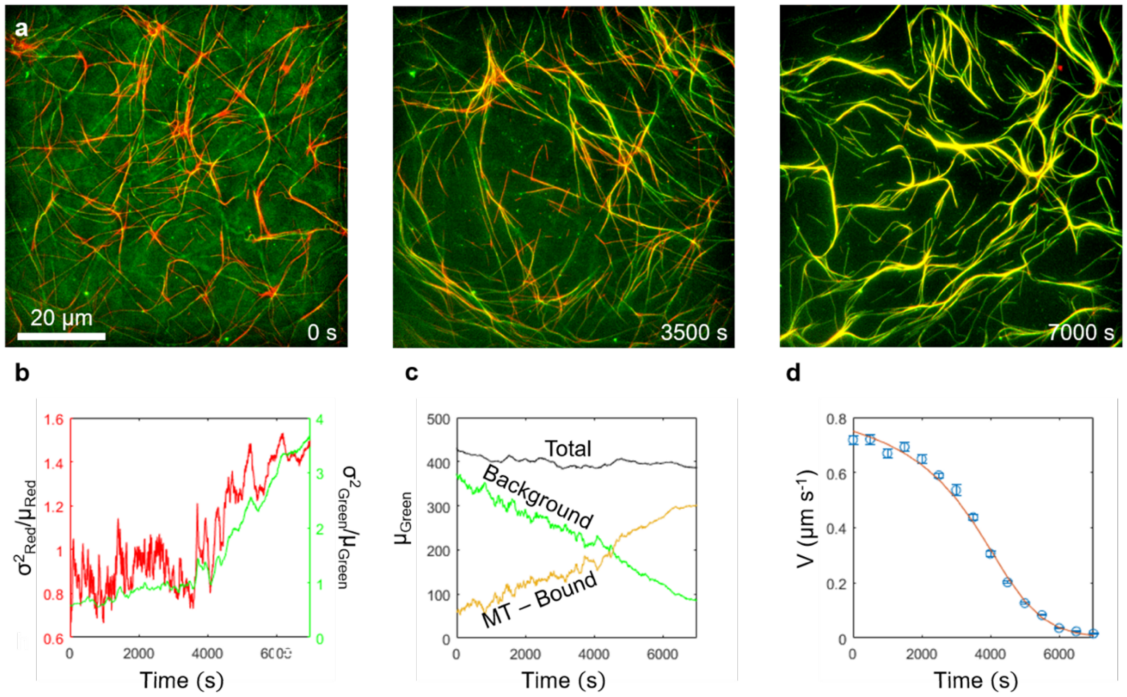

Figure 3. Microtubules assemble into bundles as GFP-kinesins assemble on microtubules. (a) Flattened composite images of microtubules gliding in the presence of an initial 10 mM ATP. (b-d) Analysis of flattened images in (a). (b) Ratio of pixel-wise variance to pixel-wise mean plotted against time. (c) Decomposition of mean green channel fluorescence into a background (green) and a microtubule-bound (orange) component, as determined by performing linear regression on green channel fluorescence as a function of red channel fluorescence. (d) Microtubule velocity with respect to time, fit with a function accounting for ATP-dependent velocity and velocity-dependent ATP depletion.

Collective microtubule behavior arises from nematic alignment

The emergence of collective behavior requires the presence of interactions between individual agents. In this system, the result of these interactions is the nematic alignment of microtubules upon collision (Figure 4a). The alignment is reversible, in that microtubules dissociate from bundles either mid bundle or at bundle turns (Figure 4b).

In previous studies of microtubules propelled by (permanently) surface-adhered full-length kinesins, a microtubule colliding with another microtubule usually passes either over or under it, likely as a result of height fluctuations of the advancing microtubule tip.[72, 73] In studies demonstrating collective behavior, filament alignment has been usually achieved by engineering interactions between filaments, either by the use of strong, streptavidin-biotin interactions,[37] depletion forces,[40] or DNA-crosslinking.[34] A recent study examining the gliding of microtubules on SNAP-tagged kinesin motors bound to a Pluronic-F127 coated surface found that tuning kinesin surface density allowed for the control of filament alignment during collisions.[41] Alignment events were occasionally observed in the previous version of our system, but were too rare to generate collective behavior.[54]

In the current system, interactions originate primarily from steric effects and chemical guidance. High densities of GFP-kinesin motors, similar to the ones that are used in this experiment (consisting of the first N-terminal 401 amino acids of kinesin from *Drosophila melanogaster* compared to the first N-terminal 430 amino acids of rat kinesin used in these experiments), have been previously shown to mechanically influence the dynamics of microtubule gliding.[69] In this dynamic system, under the chosen conditions, microtubules generate many linkages to the surface *via* the high density of kinesin motors recruited from solution. The dense surface attachment reduces vertical fluctuations and prevents microtubules from crossing each other, forcing them to buckle and align with the microtubule they are colliding with. This is supported by the observation that bundling increases as the density of microtubule-bound kinesin increases (Figure 3c). Additionally, the kinesin motors used here have truncated tails (430 amino acids) and are thus shorter than the full-length kinesin (963 amino acids for rat kinesin[74]), so they cannot be stretched as much to accommodate a crossover.

In further support of the concept that steric interactions are a source of nematic alignment among microtubules, we were able to observe 'ramming' events, where an incoming microtubule visibly indents another microtubule (Figure 4c). However, such microtubule deflections are rare; we were only able to observe a few such events in experiments initialized with 1 mM ATP. This is not surprising, since typically more kinesins hold the indented microtubules

than push the ramming microtubule. However, visible deflections become more frequent if microtubules are gliding in the presence of 1 mM AMP-PNP (the non-hydrolyzable analog of ATP, adenylyl-imidodiphosphate). An example of this is shown in Figure 4c. AMP-PNP molecules lock kinesin motors in their strong microtubule-binding state, which increases the density of kinesin motors holding the microtubule to the surface, and most likely acts as a support to prevent microtubules from buckling early, thereby facilitating 'ramming' events.

"Snapping into alignment" contributes to bundle formation

An additional mechanism by which microtubules align is a 'snapping' event, where a microtubule that has begun to cross over another microtubule suddenly snaps to align with the microtubule it has crossed over (Figure 4d). This "snapping into alignment" has been observed in Brownian Dynamics simulations of gliding microtubules approaching the edge of a kinesin-track,[75] and can be considered chemical guiding by the kinesin track formed under a gliding microtubule.

A phenomenon similar to "snapping into alignment" has been observed in microtubules growing in the presence of the positively charged tetravalent starPEG-$(KA_7)_4$ cross-linker that was designed to mimic microtubule associated proteins.[76] This cross-linker, which has a dissociation constant for a microtubule of 30 nM, was found to laterally zip microtubules at cross-linker concentrations of 50 nM and 100 nM. In addition, when concentrated at the depolymerizing end of a microtubule, this cross-linker was found to produce depolymerization-coupled forces of up to 8.4 pN. Although it is likely that multi-valent kinesin motors are present in our dynamic system (discussed below), it is unlikely that the same zippering mechanism plays a significant role during snapping events, as these happen on a much faster time scale. The data shown by Drechsler *et al.*[76] suggests that zippering events happen over the course of 40-50 s, while the snapping events observed here occur in under 5 s.

Chemical guiding by the kinesin trail: The case for pheromonic interactions

Prior work on filament guiding on motor protein coated surfaces has shown that filaments follow permanent trails of motors created by chemical surface patterning if the required change in the angle of motion is small ($<15^0$ for microtubules),[75, 77, 78] or if the microtubule is already aligned with a narrow track and the radius of curvature is large enough (> 17 μm).[80] Trails of motors have also been printed by deposition of motor-covered microtubules; these extremely narrow tracks have a length equal to the depositing microtubule, guide movements effectively, and can be considered a "static" precursor to the dynamic attachment introduced by us.[79]

These "chemical guiding" mechanisms imply that the deposition of a kinesin trail by one microtubule may induce another microtubule to follow, which would be reminiscent of the trails of pheromones deposited by ants to induce other ants to follow and it would constitute another, "pheromonic" interaction mechanism between gliding microtubules.

Such pheromonic interactions were weak in our previous work using low microtubule densities,[54, 55] because it was exceedingly rare that a gliding microtubule encounters a kinesin trail under a small enough angle. In the system described here, the initially high density of kinesins on the surface makes the kinesin trails less prominent and prevents alignment. However, steric interactions can align microtubules and the redistribution of the kinesin motors from the surface to the trails (Fig. 3a) can increase the prominence of the kinesin trails relative to the surrounding surface, resulting in a strengthening of the pheromonic interaction. An example of a microtubule behavior potentially related to the pheromonic interaction is shown in Supplementary Section 10, where a microtubule begins to migrate away from another microtubule but soon returns to rejoin it. We initially interpreted the absence of microtubules emerging from the outside of a curved bundle as indication that the bundle must be stabilized by depletion forces (absent here, see next section), cross-linkers (weak here, see next section), or a pheromonic interaction. However, the bundle morphology observed by Tanida *et al.*[41] in the absence of the pheromonic interaction (Fig. 1a) appears identical to the bundle morphology in our system (Fig. 1d), demonstrating that a pheromonic interaction is not required to explain the system behavior.

Alternative mechanisms of microtubule interactions

There are two other conceivable mechanisms by which microtubules interact in our assay: (1) depletion forces induced by excess Pluronic F108-NTA remaining in solution and (2) multi-headed kinesin motors cross-linking to each other in solution and then cross-linking microtubules. However, for the reasons outlined below, we do not believe these mechanisms play a significant role.

Previous studies have reported that the generation of depletion forces in systems of active nanoscale filaments require polymer concentrations on the order of a few milligrams per milliliter. For example, the work of Inoue *et al.*[40] used a concentration of 3 mg/mL methylcellulose to induce depletion forces in a classical motility assay, and the work of Wu *et al.*[81] used 20 mg/mL of Pluronic F127. In our experiments, while we do initially flow in 20 μL of 2 mg/mL Pluronic F108-NTA to coat the surface of the flow chamber, we then wash it out three times with 20 μL of BRB80 buffer. This suggests that the leftover Pluronic F108-NTA concentration can be expected to be as much as three orders of magnitude lower than that required for inducing depletion forces between microtubules[82]. Furthermore, the presence of depletion forces would have a constant effect on nematic alignment, which is in contrast to the velocity-dependent alignment that is observed in this dynamic system. As a result, we conclude that the Pluronic F108-NTA polymer remaining in solution is insufficient to cause significant depletion forces.

Microtubules can also interact by cross-linking *via* kinesins. This can be seen from the formation of dense microtubule clusters when microtubules and kinesin are mixed in the presence of 1 mM ATP and either 100 μM or 1 mM AMP-PNP, which locks kinesin motors in a strong microtubule-binding state. It is possible that these cross links contribute to microtubule interactions. Indeed, cross-linkers such as Ase1 have been found to generate significantly stronger entropic sliding forces between microtubules than the depletion forces which have been used for generating collective behavior.[83-85] However, it is also important to note that, in our experiments, even at high AMP-PNP concentrations, the cross-links are reversible and do not significantly affect microtubule velocity. In Supplementary Section 11, we demonstrate that a cluster of microtubules can spread out over time. In Supplementary Section 12, we show that microtubules gliding in the presence of 1 mM AMP-PNP (while moving significantly slower overall) do not exhibit a statistically significant change in velocity even during antiparallel collisions.

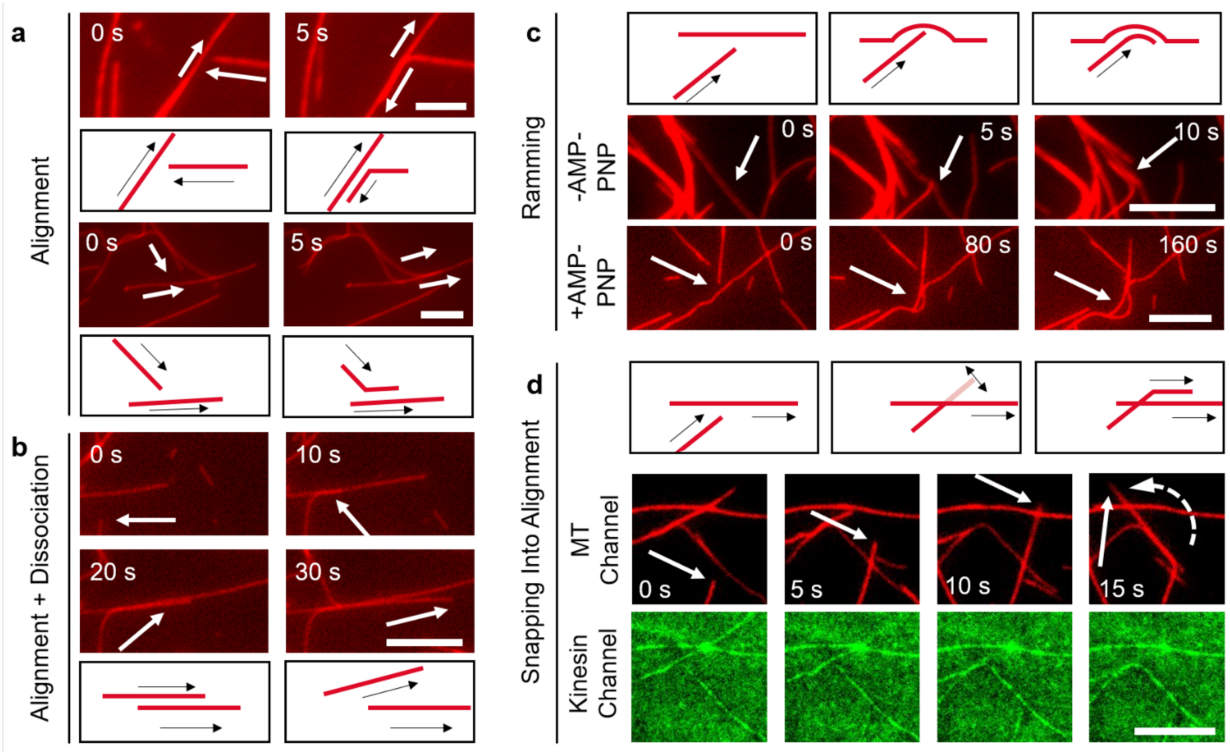

Figure 4. Microtubule interactions. (a) Collisions do not lead to crossing but to alignment either in antiparallel or parallel fashion depending on the angle of collision. Scale bar: 5 μm (Top), 10 μm (Bottom). (b) The alignment is reversible, as microtubules can dissociate afterwards. Scale bar: 10 μm. (c) A microtubule "ramming" another microtubule and creating an indent in the absence (top) and presence (bottom) of AMP-PNP. Scale bar: 10 μm (Top and Bottom). (d) Microtubule "snapping" to align with another microtubule that it had already crossed. Scale bar: 20 μm.

The origin of these kinesin cross-links is unclear. A likely explanation is that motors aggregate, generating multi-headed complexes that can bind multiple microtubules at once. An alternative, though unlikely, mechanism for multivalent kinesin formations is nickel ion mediated interactions of their His-tags.[86] In our experiments, it is unlikely that this mechanism plays a major role because it requires free nickel ions in solution. However, nickel ion chelating agents (NTA groups on the surface and 2 mM EGTA in the BRB80 buffer) will bind all free nickel ions and compete them away from the His-tags. In addition, such cross-linking would prevent microtubules from dissociating after aligning, which is not what we observe (Figure 4b).

Comparison of collective behavior to other dynamic systems

The bundles formed in our dynamic system are similar to the active foam generated in numerical simulations of Vicsek-like particles moving with memory.[87] They are also similar to the swirling, spooling, and giant flock regimes generated in simulations of gliding filaments with high rigidities and interaction energies.[88] Tanida *et al.*[41] recently investigated the effects of tunable binary collisions in a dynamic system where the strength of the microtubule-surface bond is regulated by kinesin density, and found that increasing bond strength changed the system behavior from long range order to aggregation. The bundles formed in their system at moderate kinesin surface density (example shown in Fig. 1a) are similar to the bundles generated in our dynamic system.

Conclusions

In this study, we present a system of two agents exhibiting mutualistic collective motion where components dynamically rearrange to maximize system utility: microtubules assemble into dense bundles and kinesin motors rearrange to support the assembled bundles. These bundles have several layers of dynamic organization: first, kinesin motors are assembled by single microtubules to allow for microtubule propulsion; next, propelled microtubules collide and align due to the strong surface bond provided by the kinesin motors (the first level of organization), forming long bundles; finally, bundles interact to form large scale networks stabilized by the migration of the kinesin from the surface to the trails. Swarming is thus achieved here through a combination of direct, steric interactions and environmental modification (the assembly of kinesins into trails on the surface).

The high degree of engagement (>95%) of the available kinesin motors in the generation of force, as indicated by the rapid consumption of ATP and the depletion of the kinesin from the surface areas between trails, is a highly desirable outcome. Dynamic turnover enables adaptation and self-repair, but ideally unproductive stores of building blocks are kept small. This has been achieved here by increasing the surface affinity for kinesin motors, which reduced the concentration of motors in the solution without impeding the kinesin trail formation.

The next steps will aim to achieve unidirectional movement of the microtubules in these bundles, for example through the utilization of asymmetric guiding structures, as well as the coupling of loads to the microtubules in the bundles to extract work from the system. Ultimately, this work pushes towards the development of artificial muscles from active nanoscale filaments.

Methods

Microtubule and Kinesin Preparation. Microtubules were polymerized by reconstituting 10 μg of HiLyte647-labeled lyophilized tubulin (Cytoskeleton Inc., Denver, CO) in 6.25 μL of polymerization buffer (BRB80 buffer and 4 mM $MgCl_2$, 1 mM GTP, 5% dimethyl sulfoxide) and incubating at 37 °C for 75 min. BRB80 buffer contains 80 mM piperazine-N,N′-bis(2ethanesulfonic acid), 1 mM $MgCl_2$, and 1 mM ethylene glycol tetraacetic acid at a pH of 6.9 (adjusted with KOH). The microtubules were then stabilized by diluting them 20-fold into BRB80 buffer with 10 μM paclitaxel (Sigma, Saint Louis, MO). A kinesin construct containing the first 430 amino acids of rat kinesin heavy chain fused to eGFP and a C-terminal His-tag at the tail domain (rkin430eGFP)[89] was expressed in Escherichia coli and purified using a Ni−NTA column (prepared by the team of G. Bachand at the Center for Integrated Nanotechnologies at Sandia National Laboratories). The concentration of the GFP-kinesin stock solution was 2.5 μM as determined by observing the absorbance at 488 nm with a Nanodrop instrument with a 1 mm path length.

Surface cleaning. Coverslips were cleaned by sonicating them for 20 minutes in acetone, rinsing with water, sonicating for 20 min in 1 M KOH, rinsing with water, and oven-drying. The dried coverslips were then UV/ozone treated on both sides for 20 min, sonicated in water for 20 min, and oven dried. The coverslips were then UV/ozone treated again, after which they were immersed in a solution of 5% dimethyldichlorosilane in toluene for 30 min. Coverslips were then rinsed two times with toluene, three times with methanol, and dried with nitrogen gas.

Experimental procedure. Cleaned coverslips were assembled into a flow cell of 1 cm width and 100 μm height using double-sided tape as spacers. A solution of 2 mg/mL Pluronic F108-NTA (gift from AllVivo Vascular) in 500 mM nickel(II) sulfate (Sigma, Saint Louis, MO) was first flowed into the flow cell. The Pluronic-F108-NTA was allowed to adsorb for 7 min. Then the solution was replaced three times with 15 μL BRB80 buffer solution. Next, a solution containing microtubules (8 μg mL^{-1}), 25 nM GFP-kinesin, 1 mM ATP in 0.5 mg/mL casein (Sigma), 10 μM paclitaxel, and an enzymatic antifade system (20 mM D-glucose, 20 μg mL^{-1} glucose oxidase, and 8 μg mL^{-1} catalase) in BRB80 buffer was flown in. The edges of the flow cell were sealed with vacuum grease to prevent evaporation.

Images were acquired with an objective-type total internal reflection fluorescence setup on an Eclipse Ti microscope (Nikon Instruments, Melville, NY) with a 100×/1.49 NA objective lens (Nikon Instruments, Melville, NY) using a 642 nm laser and a 480 nm laser (Omicron Laserage) for the imaging of microtubules and kinesin, respectively. Pairs of images were taken with a Zyla 4.2 sCMOS camera (Andor Technology) once every 5 s (exposure time of 30 ms for both channels) for as long as motility was observed. All experiments were performed at room temperature, which varied between 22-24 °C.

Supporting Information

The Supporting Information is available free of charge on the ACS Publications website:

The supporting sections referenced in the main text, including (1) kinesin fluorescence calibration, (2) models for the kinesin-surface interaction, (3) kinesin fluorescence profile over the course of two hours, (4) FRAP experiment analysis, (5) single molecule analysis of the kinesin-surface interaction, (6) analysis of microtubule gliding assays, (7) kinesin dwell time analysis on microtubules, (8) effect of the addition of AMP-PNP to the microtubule gliding assay, (9) effect of changing kinesin/microtubule concentration, (10) example of a possible pheromonic interaction, (11) dispersion of AMP-PNP-induced microtubule cluster, and (12) change in MT velocity during collisions in the presence of AMP-PNP.

Acknowledgements

The authors thank G. Bachand for providing the GFP-kinesin protein. This work was performed, in part, at the Center for Integrated Nanotechnologies, an Office of Science User

Facility operated for the US Department of Energy (DOE) Office of Science by Los Alamos National Laboratory (contract no. DE- AC52-06NA25396) and Sandia National Laboratories (contract no. 97 DE-AC04-94AL85000). The authors thank Dr. Jennifer Neff and AllVivo Vascular for their gift of Pluronic-F108 functionalized with NTA. Financial support by the National Science Foundation Division of Materials Research under Grant No. 1807514 is gratefully acknowledged.

References:

1. Sumpter, D. J. T., The Principles of Collective Animal Behaviour. *Philos. Trans. R. Soc. B* **2006,** *361*, 5-22.
2. Gilbert, C.; Robertson, G.; Le Maho, Y.; Naito, Y.; Ancel, A., Huddling Behavior in Emperor Penguins: Dynamics of Huddling. *Physiol. Behav.* **2006,** *88*, 479-488.
3. Fretwell, P. T.; LaRue, M. A.; Morin, P.; Kooyman, G. L.; Wienecke, B.; Ratcliffe, N.; Fox, A. J.; Fleming, A. H.; Porter, C.; Trathan, P. N., An Emperor Penguin Population Estimate: The First Global, Synoptic Survey of a Species from Space. *PLoS One* **2012,** *7*, e33751.
4. Deutsch, A.; Theraulaz, G.; Vicsek, T., Collective Motion in Biological Systems. *Interface Focus* **2012,** *2*, 689-692.
5. Vicsek, T.; Czirók, A.; Ben-Jacob, E.; Cohen, I.; Shochet, O., Novel Type of Phase Transition in a System of Self-Driven Particles. *Phys. Rev. Lett.* **1995,** *75*, 1226-1229.
6. Ballerini, M.; Cabibbo, N.; Candelier, R.; Cavagna, A.; Cisbani, E.; Giardina, I.; Lecomte, V.; Orlandi, A.; Parisi, G.; Procaccini, A.; Viale, M.; Zdravkovic, V., Interaction Ruling Animal Collective Behavior Depends on Topological Rather Than Metric Distance: Evidence from a Field Study. *Proc. Natl. Acad. Sci. U. S. A.* **2008,** *105*, 1232-1237.
7. Vicsek, T.; Zafeiris, A., Collective Motion. *Phys. Rep.* **2012,** *517*, 71-140.
8. Rubenstein, M.; Cornejo, A.; Nagpal, R., Programmable Self-Assembly in a Thousand-Robot Swarm. *Science* **2014,** *345*, 795.
9. Werfel, J.; Petersen, K.; Nagpal, R., Designing Collective Behavior in a Termite-Inspired Robot Construction Team. *Science* **2014,** *343*, 754.
10. Yang, G.-Z.; Bellingham, J.; Dupont, P. E.; Fischer, P.; Floridi, L.; Full, R.; Jacobstein, N.; Kumar, V.; McNutt, M.; Merrifield, R.; Nelson, B. J.; Scassellati, B.; Taddeo, M.; Taylor, R.; Veloso, M.; Wang, Z. L.; Wood, R., The Grand Challenges of Science Robotics. *Sci. Robot.* **2018,** *3*, eaar7650.
11. Schuerle, S.; Soleimany, A. P.; Yeh, T.; Anand, G. M.; Häberli, M.; Fleming, H. E.; Mirkhani, N.; Qiu, F.; Hauert, S.; Wang, X.; Nelson, B. J.; Bhatia, S. N., Synthetic and Living Micropropellers for Convection-Enhanced Nanoparticle Transport. *Sci. Adv.* **2019,** *5*, eaav4803.
12. Li, J.; Angsantikul, P.; Liu, W.; Esteban-Fernández de Ávila, B.; Chang, X.; Sandraz, E.; Liang, Y.; Zhu, S.; Zhang, Y.; Chen, C.; Gao, W.; Zhang, L.; Wang, J., Biomimetic Platelet-Camouflaged Nanorobots for Binding and Isolation of Biological Threats. *Adv. Mater.* **2018,** *30*, 1704800.
13. Palagi, S.; Fischer, P., Bioinspired Microrobots. *Nat. Rev. Mat.* **2018,** *3*, 113-124.
14. Karshalev, E.; Esteban-Fernández de Ávila, B.; Beltrán-Gastélum, M.; Angsantikul, P.; Tang, S.; Mundaca-Uribe, R.; Zhang, F.; Zhao, J.; Zhang, L.; Wang, J., Micromotor Pills as a Dynamic Oral Delivery Platform. *ACS Nano* **2018,** *12*, 8397-8405.
15. Alapan, Y.; Yasa, O.; Schauer, O.; Giltinan, J.; Tabak, A. F.; Sourjik, V.; Sitti, M., Soft Erythrocyte-Based Bacterial Microswimmers for Cargo Delivery. *Sci. Robot.* **2018,** *3*, eaar4423.
16. Felfoul, O.; Mohammadi, M.; Taherkhani, S.; de Lanauze, D.; Zhong Xu, Y.; Loghin, D.; Essa, S.; Jancik, S.; Houle, D.; Lafleur, M.; Gaboury, L.; Tabrizian, M.; Kaou, N.; Atkin, M.; Vuong, T.; Batist, G.; Beauchemin, N.; Radzioch, D.; Martel, S., Magneto-Aerotactic Bacteria Deliver Drug-Containing Nanoliposomes to Tumour Hypoxic Regions. *Nat. Nanotechnol.* **2016,** *11*, 941.
17. Wang, H.; Pumera, M., Coordinated Behaviors of Artificial Micro/Nanomachines: From Mutual Interactions to Interactions with the Environment. *ChSRv* **2020,** *49*, 3211-3230.
18. Hult, R.; Campos, G. R.; Steinmetz, E.; Hammarstrand, L.; Falcone, P.; Wymeersch, H., Coordination of Cooperative Autonomous Vehicles: Toward Safer and More Efficient Road Transportation. *IEEE Signal Process. Mag.* **2016,** *33*, 74-84.
19. Iftekhar, L.; Olfati-Saber, R. In *Autonomous Driving for Vehicular Networks with Nonlinear Dynamics*, 2012 IEEE Intelligent Vehicles Symposium, 3-7 June 2012; 2012; pp 723-729.
20. Kushleyev, A.; Mellinger, D.; Powers, C.; Kumar, V., Towards a Swarm of Agile Micro Quadrotors. *Auton. Robots* **2013,** *35*, 287-300.
21. Hess, H.; Clemmens, J.; Qin, D.; Howard, J.; Vogel, V., Light-Controlled Molecular Shuttles Made from Motor Proteins Carrying Cargo on Engineered Surfaces. *Nano Lett.* **2001,** *1*, 235-239.
22. Dennis, J. R.; Howard, J.; Vogel, V., Molecular Shuttles: Directed Motion of Microtubules Along Nanoscale Kinesin Tracks. *Nanotechnology* **1999,** *10*, 232-236.
23. Brunner, C.; Wahnes, C.; Vogel, V., Cargo Pick-up from Engineered Loading Stations by Kinesin Driven Molecular Shuttles. *Lab Chip* **2007,** *7*, 1263-1271.
24. Hess, H.; Howard, J.; Vogel, V., A Piconewton Forcemeter Assembled from Microtubules and Kinesins. *Nano Lett.* **2002,** *2*, 1113-1115.
25. Isozaki, N.; Shintaku, H.; Kotera, H.; Hawkins, T. L.; Ross, J. L.; Yokokawa, R., Control of Molecular Shuttles by Designing Electrical and Mechanical Properties of Microtubules. *Sci. Robot.* **2017,** *2*, eaan4882.
26. Tsitkov, S.; Hess, H., Rise of the Nanorobots: Advances in Control, Molecular Detection, and Nanoscale Actuation Are Bringing Us Closer to a New Era of Technology Enhanced by Nanorobots. *IEEE Pulse* **2017,** *8*, 23-25.
27. Bachand, G. D.; Rivera, S. B.; Boal, A. K.; Gaudioso, J.; Liu, J.; Bunker, B. C., Assembly and Transport of Nanocrystal Cdse Quantum Dot Nanocomposites Using Microtubules and Kinesin Motor Proteins. *Nano Lett.* **2004,** *4*, 817-821.
28. Bachand, G. D.; Rivera, S. B.; Carroll-Portillo, A.; Hess, H.; Bachand, M., Active Capture and Transport of Virus Particles Using a Biomolecular Motor-Driven, Nanoscale Antibody Sandwich Assay. *Small* **2006,** *2*, 381-385.
29. Fischer, T.; Agarwal, A.; Hess, H., A Smart Dust Biosensor Powered by Kinesin Motors. *Nat. Nanotechnol.* **2009,** *4*, 162.
30. Keber, F. C.; Loiseau, E.; Sanchez, T.; DeCamp, S. J.; Giomi, L.; Bowick, M. J.; Marchetti, M. C.; Dogic, Z.; Bausch, A. R., Topology and Dynamics of Active Nematic Vesicles. *Science* **2014,** *345*, 1135.

31. Sanchez, T.; Welch, D.; Nicastro, D.; Dogic, Z., Cilia-Like Beating of Active Microtubule Bundles. *Science* **2011,** *333*, 456.
32. Schaller, V.; Weber, C. A.; Hammerich, B.; Frey, E.; Bausch, A. R., Frozen Steady States in Active Systems. *Proc. Natl. Acad. Sci. U. S. A.* **2011,** *108*, 19183.
33. Huber, L.; Suzuki, R.; Krüger, T.; Frey, E.; Bausch, A. R., Emergence of Coexisting Ordered States in Active Matter Systems. *Science* **2018,** *361*, 255.
34. Keya, J. J.; Suzuki, R.; Kabir, A. M. R.; Inoue, D.; Asanuma, H.; Sada, K.; Hess, H.; Kuzuya, A.; Kakugo, A., DNA-Assisted Swarm Control in a Biomolecular Motor System. *Nat. Commun.* **2018,** *9*, 453.
35. Keya, J. J.; Kabir, A. M. R.; Inoue, D.; Sada, K.; Hess, H.; Kuzuya, A.; Kakugo, A., Control of Swarming of Molecular Robots. *Sci. Rep.* **2018,** *8*, 11756.
36. Islam, M. S.; Kuribayashi-Shigetomi, K.; Kabir, A. M. R.; Inoue, D.; Sada, K.; Kakugo, A., Role of Confinement in the Active Self-Organization of Kinesin-Driven Microtubules. *Sens. Actuators B Chem.* **2017,** *247*, 53-60.
37. Hess, H.; Clemmens, J.; Brunner, C.; Doot, R.; Luna, S.; Ernst, K.-H.; Vogel, V., Molecular Self-Assembly of "Nanowires" and "Nanospools" Using Active Transport. *Nano Lett.* **2005,** *5*, 629-633.
38. Idan, O.; Lam, A.; Kamcev, J.; Gonzales, J.; Agarwal, A.; Hess, H., Nanoscale Transport Enables Active Self-Assembly of Millimeter-Scale Wires. *Nano Lett.* **2012,** *12*, 240-245.
39. Saito, A.; Farhana, T. I.; Kabir, A. M. R.; Inoue, D.; Konagaya, A.; Sada, K.; Kakugo, A., Understanding the Emergence of Collective Motion of Microtubules Driven by Kinesins: Role of Concentration of Microtubules and Depletion Force. *RSC Adv.* **2017,** *7*, 13191-13197.
40. Inoue, D.; Mahmot, B.; Kabir, A. M. R.; Farhana, T. I.; Tokuraku, K.; Sada, K.; Konagaya, A.; Kakugo, A., Depletion Force Induced Collective Motion of Microtubules Driven by Kinesin. *Nanoscale* **2015,** *7*, 18054-18061.
41. Tanida, S.; Furuta, K. y.; Nishikawa, K.; Hiraiwa, T.; Kojima, H.; Oiwa, K.; Sano, M., Gliding Filament System Giving Both Global Orientational Order and Clusters in Collective Motion. *Phys. Rev. B.* **2020,** *101*, 032607.
42. Sanchez, T.; Chen, D. T. N.; DeCamp, S. J.; Heymann, M.; Dogic, Z., Spontaneous Motion in Hierarchically Assembled Active Matter. *Nature* **2012,** *491*, 431-434.
43. Sumino, Y.; Nagai, K. H.; Shitaka, Y.; Tanaka, D.; Yoshikawa, K.; Chaté, H.; Oiwa, K., Large-Scale Vortex Lattice Emerging from Collectively Moving Microtubules. *Nature* **2012,** *483*, 448.
44. VanDelinder, V.; Brener, S.; Bachand, G. D., Mechanisms Underlying the Active Self-Assembly of Microtubule Rings and Spools. *Biomacromolecules* **2016,** *17*, 1048-1056.
45. Lam, A. T.; VanDelinder, V.; Kabir, A. M. R.; Hess, H.; Bachand, G. D.; Kakugo, A., Cytoskeletal Motor-Driven Active Self-Assembly in in Vitro Systems. *Soft Matter* **2016,** *12*, 988-997.
46. Bachand, G. D.; Bouxsein, N. F.; VanDelinder, V.; Bachand, M., Biomolecular Motors in Nanoscale Materials, Devices, and Systems. *Wires Nanomed. Nanobi.* **2014,** *6*, 163-177.
47. Schaller, V.; Weber, C.; Semmrich, C.; Frey, E.; Bausch, A. R., Polar Patterns of Driven Filaments. *Nature* **2010,** *467*, 73-77.
48. Peet, D. R.; Burroughs, N. J.; Cross, R. A., Kinesin Expands and Stabilizes the Gdp-Microtubule Lattice. *Nat. Nanotechnol.* **2018,** *13*, 386-391.
49. Reuther, C.; Diego, A. L.; Diez, S., Kinesin-1 Motors Can Increase the Lifetime of Taxol-Stabilized Microtubules. *Nat. Nanotechnol.* **2016,** *11*, 914-915.
50. Bronstein, J. L., The Study of Mutualism. In *Mutualism*, Oxford University Press: Oxford, 2015.
51. Wing, L. D.; Buss, I. O., Elephants and Forests. *Wildlife Monographs* **1970**, 3-92.
52. Blake, S.; Inkamba-Nkulu, C., Fruit, Minerals, and Forest Elephant Trails: Do All Roads Lead to Rome? *Biotropica* **2004,** *36*, 392-401.
53. Campos-Arceiz, A.; Blake, S., Megagardeners of the Forest – the Role of Elephants in Seed Dispersal. *Acta Oecol.* **2011,** *37*, 542-553.
54. Lam, A. T.-C.; Tsitkov, S.; Zhang, Y.; Hess, H., Reversibly Bound Kinesin-1 Motor Proteins Propelling Microtubules Demonstrate Dynamic Recruitment of Active Building Blocks. *Nano Lett.* **2018,** *18*, 1530-1534.
55. Bassir Kazeruni, N. M.; Tsitkov, S.; Hess, H., Assembling Molecular Shuttles Powered by Reversibly Attached Kinesins. *J. Vis. Exp.* **2019**, e59068.
56. Nieba, L.; Nieba-Axmann, S. E.; Persson, A.; Hämäläinen, M.; Edebratt, F.; Hansson, A.; Lidholm, J.; Magnusson, K.; Karlsson, Å. F.; Plückthun, A., Biacore Analysis of Histidine-Tagged Proteins Using a Chelating Nta Sensor Chip. *Anal. Biochem.* **1997,** *252*, 217-228.
57. Knecht, S.; Ricklin, D.; Eberle, A. N.; Ernst, B., Oligohis-Tags: Mechanisms of Binding to Ni2+-Nta Surfaces. *J. Mol. Recognit.* **2009,** *22*, 270-279.
58. Myszka, D. G.; He, X.; Dembo, M.; Morton, T. A.; Goldstein, B., Extending the Range of Rate Constants Available from Biacore: Interpreting Mass Transport-Influenced Binding Data. *Biophys. J.* **1998,** *75*, 583-594.
59. Schuck, P.; Zhao, H., The Role of Mass Transport Limitation and Surface Heterogeneity in the Biophysical Characterization of Macromolecular Binding Processes by Spr Biosensing. In *Surface Plasmon Resonance: Methods and Protocols*, Mol, N. J.; Fischer, M. J. E., Eds. Humana Press: Totowa, NJ, 2010; pp 15-54.
60. Miura, T.; Seki, K., Diffusion Influenced Adsorption Kinetics. *J. Phys. Chem. B* **2015,** *119*, 10954-10961.
61. Chang, Y.; Chu, W.-L.; Chen, W.-Y.; Zheng, J.; Liu, L.; Ruaan, R.-C.; Higuchi, A., A Systematic Spr Study of Human Plasma Protein Adsorption Behavior on the Controlled Surface Packing of Self-Assembled Poly(Ethylene Oxide) Triblock Copolymer Surfaces. *J. Biomed. Mater. Res. A* **2010,** *93A*, 400-408.
62. Bhagawati, M.; Ghosh, S.; Reichel, A.; Froehner, K.; Surrey, T.; Piehler, J., Organization of Motor Proteins into Functional Micropatterns Fabricated by a Photoinduced Fenton Reaction. *Angew. Chem. Int. Ed.* **2009,** *48*, 9188-9191.
63. Lata, S.; Reichel, A.; Brock, R.; Tampé, R.; Piehler, J., High-Affinity Adaptors for Switchable Recognition of Histidine-Tagged Proteins. *J. Am. Chem. Soc.* **2005,** *127*, 10205-10215.
64. Sitt, A.; Hess, H., Directed Transport by Surface Chemical Potential Gradients for Enhancing Analyte Collection in Nanoscale Sensors. *Nano Lett.* **2015,** *15*, 3341-3350.
65. Walder, R.; Nelson, N.; Schwartz, D. K., Single Molecule Observations of Desorption-Mediated Diffusion at the Solid-Liquid Interface. *Phys. Rev. Lett.* **2011,** *107*.

66. Nitta, T.; Hess, H., Dispersion in Active Transport by Kinesin-Powered Molecular Shuttles. *Nano Lett.* **2005,** *5*, 1337-1342.
67. Narayan, V.; Ramaswamy, S.; Menon, N., Long-Lived Giant Number Fluctuations in a Swarming Granular Nematic. *Science* **2007,** *317*, 105-108.
68. Schief, W. R.; Clark, R. H.; Crevenna, A. H.; Howard, J., Inhibition of Kinesin Motility by Adp and Phosphate Supports a Hand-over-Hand Mechanism. *Proc. Natl. Acad. Sci. U. S. A.* **2004,** *101*, 1183-8.
69. Bieling, P.; Telley, I. A.; Piehler, J.; Surrey, T., Processive Kinesins Require Loose Mechanical Coupling for Efficient Collective Motility. *EMBO Rep.* **2008,** *9*, 1121-1127.
70. Rank, M.; Frey, E., Crowding and Pausing Strongly Affect Dynamics of Kinesin-1 Motors Along Microtubules. *Biophys. J.* **2018,** *115*, 1068-1081.
71. Alonso, M. C.; Drummond, D. R.; Kain, S.; Hoeng, J.; Amos, L.; Cross, R. A., An Atp Gate Controls Tubulin Binding by the Tethered Head of Kinesin-1. *Science* **2007,** *316*, 120-123.
72. Kerssemakers, J.; Ionov, L.; Queitsch, U.; Luna, S.; Hess, H.; Diez, S., 3d Nanometer Tracking of Motile Microtubules on Reflective Surfaces. *Small* **2009,** *5*, 1732-1737.
73. Boal, A. K.; Bachand, G. D.; Rivera, S. B.; Bunker, B. C., Interactions between Cargo-Carrying Biomolecular Shuttles. *Nanotechnology* **2005,** *17*, 349-354.
74. Consortium, T. U., Uniprot: A Worldwide Hub of Protein Knowledge. *Nucleic Acids Res.* **2018,** *47*, D506-D515.
75. Ishigure, Y.; Nitta, T., Understanding the Guiding of Kinesin/Microtubule-Based Microtransporters in Microfabricated Tracks. *Langmuir* **2014,** *30*, 12089-12096.
76. Drechsler, H.; Xu, Y.; Geyer, V. F.; Zhang, Y.; Diez, S., Multivalent Electrostatic Microtubule Interactions of Synthetic Peptides Are Sufficient to Mimic Advanced Map-Like Behavior. *Mol. Biol. Cell* **2019,** *30*, 2953-2968.
77. Nicolau, D. V.; Suzuki, H.; Mashiko, S.; Taguchi, T.; Yoshikawa, S., Actin Motion on Microlithographically Functionalized Myosin Surfaces and Tracks. *Biophys. J.* **1999,** *77*, 1126-34.
78. Clemmens, J.; Hess, H.; Lipscomb, R.; Hanein, Y.; Böhringer, K. F.; Matzke, C. M.; Bachand, G. D.; Bunker, B. C.; Vogel, V., Mechanisms of Microtubule Guiding on Microfabricated Kinesin-Coated Surfaces: Chemical and Topographic Surface Patterns. *Langmuir* **2003,** *19*, 10967-10974.
79. Reuther, C.; Hajdo, L.; Tucker, R.; Kasprzak, A. A.; Diez, S., Biotemplated Nanopatterning of Planar Surfaces with Molecular Motors. *Nano Lett.* **2006,** *6*, 2177-2183.
80. Reuther, C.; Mittasch, M.; Naganathan, S. R.; Grill, S. W.; Diez, S., Highly-Efficient Guiding of Motile Microtubules on Non-Topographical Motor Patterns. *Nano Lett.* **2017,** *17*, 5699-5705.
81. Wu, K.-T.; Hishamunda, J. B.; Chen, D. T. N.; DeCamp, S. J.; Chang, Y.-W.; Fernández-Nieves, A.; Fraden, S.; Dogic, Z., Transition from Turbulent to Coherent Flows in Confined Three-Dimensional Active Fluids. *Science* **2017,** *355*, eaal1979.
82. Howard, J.; Hunt, A. J.; Baek, S., Chapter 10 Assay of Microtubule Movement Driven by Single Kinesin Molecules. In *Methods Cell Biol.*, Scholey, J. M., Ed. Academic Press: 1993; Vol. 39, pp 137-147.
83. Hilitski, F.; Ward, A. R.; Cajamarca, L.; Hagan, M. F.; Grason, G. M.; Dogic, Z., Measuring Cohesion between Macromolecular Filaments One Pair at a Time: Depletion-Induced Microtubule Bundling. *Phys. Rev. Lett.* **2015,** *114*, 138102.
84. Inoue, D.; Mahmot, B.; Kabir, A. M. R.; Farhana, T. I.; Tokuraku, K.; Sada, K.; Konagaya, A.; Kakugo, A., Depletion Force Induced Collective Motion of Microtubules Driven by Kinesin. *Nanoscale* **2015,** *7*, 18054-18061.
85. Braun, M.; Diez, S.; Lansky, Z., Cytoskeletal Organization through Multivalent Interactions. *J. Cell Sci.* **2020,** *133*, jcs234393.
86. Surrey, T.; Nédélec, F.; Leibler, S.; Karsenti, E., Physical Properties Determining Self-Organization of Motors and Microtubules. *Science* **2001,** *292*, 1167-1171.
87. Nagai, K. H.; Sumino, Y.; Montagne, R.; Aranson, I. S.; Chaté, H., Collective Motion of Self-Propelled Particles with Memory. *Phys. Rev. Lett.* **2015,** *114*, 168001.
88. Moore, J. M.; Thompson, T. N.; Glaser, M.; Betterton, M. D., Collective Motion of Driven Semiflexible Filaments Tuned by Soft Repulsion and Stiffness. *Soft Matter* **2020**.
89. Rogers, K. R.; Weiss, S.; Crevel, I.; Brophy, P. J.; Geeves, M.; Cross, R., Kif1d Is a Fast Non-Processive Kinesin That Demonstrates Novel K-Loop-Dependent Mechanochemistry. *EMBO J.* **2001,** *20*, 5101-5113.